

Sorption Properties of Methyl Orange
onto Chemically Modified Chitosan:
Thermodynamics and Kinetics StudiesJuliana CM Cajé, Paula Marcelle de Oliveira, Felipe S Semaan, Raphael C Cruz,
Ricardo J. Cassella and Wagner F. Pacheco**Department of Analytical Chemistry, Federal Fluminense University, Brazil*

Article Information

Received date: Oct 24, 2016

Accepted date: Dec 26, 2016

Published date: Jan 03, 2017

*Corresponding author

Wagner F. Pacheco, Department of
Analytical Chemistry, Federal Fluminense
University, Brazil, Email: wfpacheco@
id.uff.brDistributed under Creative Commons
CC-BY 4.0**Keywords** Sorption; Kinetics studies;
Chitosan; Cross-linked chitosan;
Epichlorohydrin; Dye removal

Abstract

A new kind of sorbent with high adsorption capacity and stability was prepared using chitosan and epichlorohydrin through a cross-linking reaction and assessed by using methyl orange. The sorption capability was evaluated by means of kinetics and equilibrium studies. Relevant factors for such sorption process were also assessed. After optimization of the relevant sorption factors, the percentages for methyl orange removal by chitosan and by modified chitosan were 82%, and 67%, respectively. Although the cross-linked chitosan offered the lowest removal percentage, this sorbent presented other relevant advantages when compared to non-modified chitosan, such as higher chemical and thermal stabilities.

Introduction

Industrial impacts on environmental resources, especially natural water, have been among the most relevant problems in our society in the last few decades. In this context, industrial activity is responsible for generating large amounts of wastewater [1]. Such complex waste presents a varied composition, depending on the type of production, and is responsible for introducing many different species and compounds in the environment, such as toxic metals, chlorinated organic substances and dyes, among others [2].

Dyes are often present in our daily lives in many different ways, and have been used in production processes of many different industries. Because of this, they are widely found in industrial effluents. The presence of these substances in water alter fundamental water characteristics, in addition to decreasing light penetration, affecting the photosynthesis of aquatic organisms. Further more, these substances are potentially harmful to the environment and the biota, and can also accumulate in the food chain [2-4].

Different treatment strategies (physical-chemical, biological and electrochemical) have been applied to remove color from wastewater containing dyes. The main techniques described in the literature are flotation and electrocoagulation, chemical oxidation, membrane separation and techniques involving decomposition by microorganisms [3]. Some of these techniques are, however, expensive and may even cause more damage to the environment through the generation of highly toxic products, besides not being, in some cases, sufficient for color removal [4]. In this context, sorption processes have been extensively studied due to their ease of application and higher efficiency in the bleaching of such residues [5].

Activated carbon is one of the most commonly used sorbents for the removal of dyes in wastewater, and, despite its high costs and problems associated to its regeneration, this method has become very popular due to its high efficiency, leading to a growing interest in the use of alternative, lower-cost, sorbents [6,7].

Some well-established alternative sorbents include carbonaceous materials [8] clays [9,10], silicates [11,12], cake and fruit peel [13,14], bark [15-17], epicarp and mesocarp babassu [18-20], microorganisms [21,22], and natural amino polysaccharides (such as chitin, and its chemical derivatization, chitosan) [2,23-26]. Natural amino polysaccharides stand out due to their excellent sorption capacity for various pollutant classes.

In this context, chitosan rises as a promising alternative biosorbent, since its selectivity against contaminants such as metals and dyes is greater in comparison to traditional resins [2,23]. On the other hand, some limitations in its use as sorbent must be taken into account, such as the fact that it is stable only within a relatively narrow pH range, usually between 6 and 10. In an acidic medium, protonation of the amino groups may reach such a degree that chitosan becomes soluble, while degradation is observed in an alkaline environment. In general, it is of great importance to extend the working range of chitosan in acidic regions, since the protonation of amine groups,

that generates a positive charge, is the main factor responsible for the interaction mechanism of chitosan with negatively charged species [24]. Such a goal can be promptly reached by chemically modifying chitosan.

The chemical modification of chitosan has been an activity of great interest in recent years, in many different fields. Such a modification can be classified as physical or chemical, and is performed in order to enhance chemical, physical and biological properties, as well to provide new functional properties [27,28].

Chemical modification promotes cross-linking among polymer chains, consisting of bringing polymer chains together with the aid of chemicals called high reactivity cross-linking agents, thus generating polymeric networks. This type of reaction requires the presence of high reactivity functional groups in the chemical structure to be modified [28-32].

This chemical process may be influenced by both physical and chemical chitosan characteristics (degree of deacetylation, and molecular weight), reaction conditions (temperature, ionic strength and time), and the cross-linking agent used, with this agent being responsible for dictating the mechanism involved in the cross-linking process, as well as the degree of cross-linking [27].

Among the well-established cross-linking agents described in literature, glutaraldehyde and epichlorohydrin are of note. They have different cross-linking mechanisms at different reaction sites of chitosan; glutaraldehyde reacts with the amino groups present in the chitosan polymer chain, forming Schiff bases by the same mechanism described for other aldehydes, such as glyoxal, while epichlorohydrin will preferentially react with the primary alcohol hydroxyl present in the polymer backbone via a bimolecular nucleophilic substitution, as predicted by the above-mentioned proposed reaction (Figure 1) [27,28,32].

Cross-linking using glutaraldehyde, as well as other aldehydes, has the drawback of blocking amino groups, which comprise the primary adsorption sites of chitosan [24,33]. Studies comparing the dye sorption capacity for acid-modified chitosan and its derivatives and sulphuric acid using glutaraldehyde were carried out by Kamari et al. (2009) [33], and according to their results, derivatives are more chemically and physically stable when compared to the starting point materials, despite their loss of sorption capacity.

Some studies available in the literature have compared modifications using different cross-linking compounds (glutaraldehyde, epichlorohydrin and diglycidyl ether), and have demonstrated that, for dye removal, epichlorohydrin-modified chitosan stands out as the more efficient choice, since its sorption capacity greater than that obtained by using other cross-linking agents, such as glutaraldehyde and diglycidyl ether, for other derivatives [29-31,33].

In the present study, the sorption phenomena of methyl orange as a model dye onto modified chitosan were studied by different points of view, aiming to reach a better understanding and allow future applications of this molecule as sorbent in waste treatment.

Experimental

Reagents and solutions: All solutions used in this study were

suitably prepared employing analytical grade chemicals and ultra-pure water (resistivity of 18.2 M Ω at 25°C) obtained prior to use by using a Direct-Q Millipore water purifier (Massachusetts, USA): The above-mentioned raw material, chitosan, used in the adsorption tests, was obtained from Sigma-Aldrich (St. Louis, USA) and classified by the manufacturer as average in molecular weight.

Stock solutions of methyl orange dye (MO, 2.29×10^{-3} mol L $^{-1}$) were prepared from a stock solution prepared by dissolving 75 mg of the dye (PA, Vetec, Brazil) in purified water with volume made up to 100.00 mL in a volumetric flask. Such solutions were stored in glass vials, protected from light and under refrigeration.

The stock solution of Britton-Robinson buffer 4.0×10^{-2} mol L $^{-1}$ was prepared by mixing 2.30 mL of glacial acetic acid (CH $_3$ COOH, PA Vetec, Brazil), 2.30 mL of phosphoric acid (H $_3$ PO $_4$, PA Vetec, Brazil) and 2.4720 g of boric acid (H $_3$ BO $_3$, PA Caledron, Toronto, Canada), previously dissolved in 50 mL of distilled water in a volumetric flask, made up to 1.00 L. The pH was adjusted to 5, 6, 7, 8 and 10 using NaOH 6 mol L $^{-1}$ (prepared by simple dissolution of NaOH pellets in water, Vetec, Brazil).

The dye solutions employed in the sorption experiments were prepared daily, by appropriate dilutions of the stock solution. The pH of the solutions were adjusted using appropriate dilutions of the universal Britton-Robinson buffer 4.0×10^{-2} mol L $^{-1}$. In order to obtain the modified chitosan, the cross-linking reaction with epichlorohydrin (C $_3$ H $_5$ ClO, Fluka, USA) was carried out in adequate chemical media.

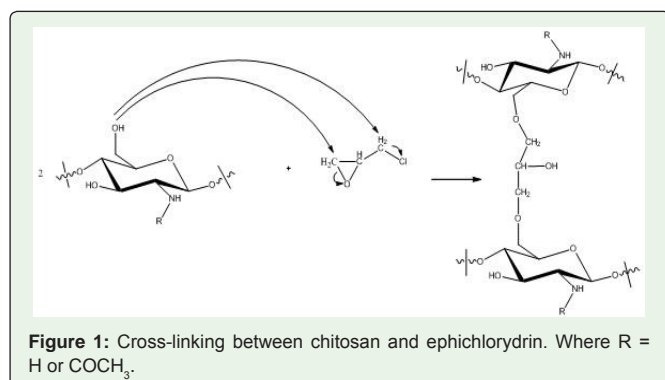
Chemical modification of chitosan: Chitosan modification using epichlorohydrin as the cross-linking reagent was conducted in homogeneous media by adapting the reaction performed by Chen et al. (2008) [27].

Approximately 5 g of the polysaccharide were solubilized using 200 mL of acetic acid 1%. The pH of the mixture was then adjusted to pH 5.0 by adding a few drops of NaOH 0.1 mol L $^{-1}$. Epichlorohydrin (12.5 mL, 0.03 mol L $^{-1}$) was slowly added to the system, and the mixture was then stirred at 50°C for 2 hours. At the end of the reaction time, the mixture was verted into 500 mL of NaOH 1.0 mol L $^{-1}$, after which precipitation of the modified polymer occurred. Subsequently, the mixture was filtered under vacuum and the chemically modified chitosan was extensively washed to remove any excess of reagents. The modified chitosan was dried in an oven at 50°C for 48hs. The solid was then grinded until the obtainment of 60 mesh-sized particles that were then used in the sorption experiments.

Preliminary characterization of the sorbents: Characterizations of both the new sorbent material (chemically-modified chitosan) and pure chitosan (raw material) were performed by IR spectrometry and Thermo Gravimetric Analyses (TGA).

Thermogravimetric curves for both sorbents were obtained using a Shimadzu DTG-60 thermogravimetric analyzer, (Japan). Analyses were performed by heating suitable amounts of each sample (circa 5 mg, in alumina open crucibles) from 35 to 1000°C at a rate of 10°C min $^{-1}$, under a dynamic nitrogen atmosphere at 50 mL min $^{-1}$ flow rate. In the case of modified chitosan, the heating was kept constant for 10 minutes at 1000°C, in order to clean the crucible and the oven.

Spectra in the infrared region were obtained on a Cary 630 infrared



spectrometer model from Agilent Technologies (São Paulo, Brazil), using infrared Fourier Transform Spectroscopy (FTIR) coupled to an Attenuated Total Reflection element (ATR). The spectra was scanned in the range of 4000-650 cm⁻¹, with 4 cm⁻¹ resolution.

The Zero Charge Point (ZCP) was defined based on the method proposed by Fiol and Villaescusa [34]. In this experiment 50 mg of adsorbent was mixed with 50mL of aqueous solution of NaCl 0,1 mol L⁻¹ in different values of initial pH (adjusted with HCl or NaOH) and let shaking for 24 hours. After this time, the final pH was measured.

Sorption studies: Adsorption experiments were carried out in batch mode, at room temperature (25-28°C) and with constant stirring, using dispersions composed of chitosan or modified chitosan particles in methyl orange dye solutions. The influence of the following parameters on the sorption process were evaluated: sorbent mass, initial pH of the solution, initial concentration of the dye and ionic strength (adjusted by buffer concentration): The experimental procedure used in the present studies obeyed the following steps: a mass of the polymer was weighed and transferred to a 50 mL polyethylene vial. Subsequently, 25.0 mL of methyl orange dye 4.58 x 10⁻⁵ mol L⁻¹ (prepared in Britton - Robinson buffer with well-defined pH and concentration) were added. The mixture was then stirred for 60 minutes at 110 rpm, and at every 2 minutes the solution was centrifuged at 5000 rpm for 3 minutes, an aliquot of the supernatant was taken and the molecular absorption spectra was registered. At the end of the measurement, the aliquot was suitably returned to the system.

The calculations and data used in the thermodynamic and kinetic simulations, which require the sorbed masses, were obtained by converting the absorbance signals into concentrations, by correlation with an analytical curve prepared on the same day.

The analytical curves were constructed by using methyl orange solutions at concentrations of 9.0 x 10⁻⁶ to 6.0 x 10⁻⁵ mol L⁻¹, prepared using buffer solutions of the same pH values used in this study. In order to do this, the appropriate volumes were transferred from the methyl orange stock solution to 10.00 mL volumetric flasks, followed by the addition of 400 μL of the respective buffer solutions. Volumes were then made up with purified water.

Extraction efficiencies were evaluated using retention percentages, which were calculated using Equation 1:

$$E(\%) = \frac{(c_i - c_t)}{c_i} \times 100 \quad (1)$$

In which C_i is the initial dye concentration in the solution, C_t is the dye concentration at time t, and E (%) is the extraction efficiency percentage.

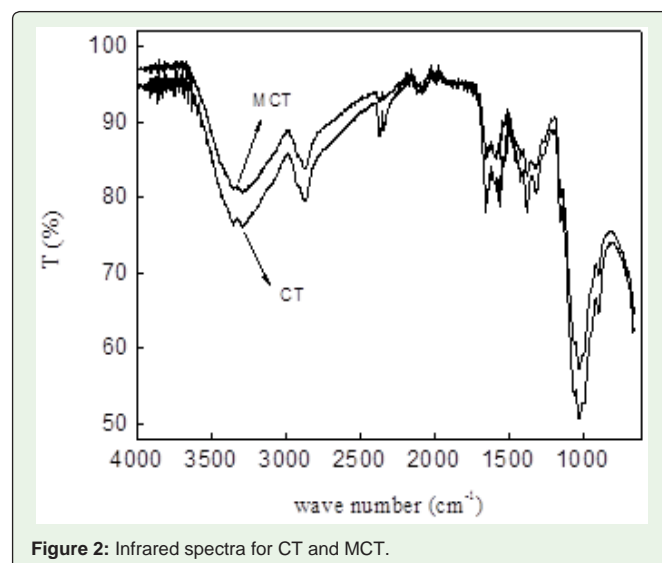
Results and Discussion

Cross-linking between chitosan and epichlorohydrin

The infrared spectra of Chitosan (CT) and Chitosan Modified With Epichlorohydrin (MCT) are displayed in (Figure 2). Both showed an intense band at 3300 cm⁻¹, related to the overlapping and vibrational stretching of the O-H and N-H bonds of the secondary amide. The band located at 2850 cm⁻¹ refers to the vibrational stretching of C-H bonds. A band at 1650 cm⁻¹, related to the angular deflection of the NH bond of the primary amine, and a vibrational stretching band for the C=O bond of the secondary amide at 1535 cm⁻¹ were also observed. The band at 1350 cm⁻¹ was assigned to the angular deformation of the C-H bonds in CH₃ groups, referring to the acetamide group also present in a small proportion in the polymer chain, since the chitosan molecule is not completely deacetylated. Finally, the band at 1025 cm⁻¹ was attributed to the vibrational stretching of the CO bond in the primary alcohol.

The differences observed in the CT and MCT IR spectra were negligible, which does not allow for concrete conclusions related to the structural changes caused by the modification. Differences found in the relative intensity of the absorption bands can be explained by the fact that the modification caused by epichlorohydrin does not introduce different functional groups or bonds when compared to those present in pure chitosan, as predicted by the proposed reaction displayed in Figure 1.

The TGA curves for Chitosan (CT) and Modified Chitosan (MCT) are shown in Figure 3. The thermogravimetric data allowed for some inferences regarding both compounds: in both cases, decomposition takes place in two stages. In the first stage, mass changes occurred probably due to the loss of water occluded within the polymer. The second stage corresponds to the decomposition of the material itself, since it is a complex process that includes deacetylation and depolymerization decomposition of the monomeric units, generating



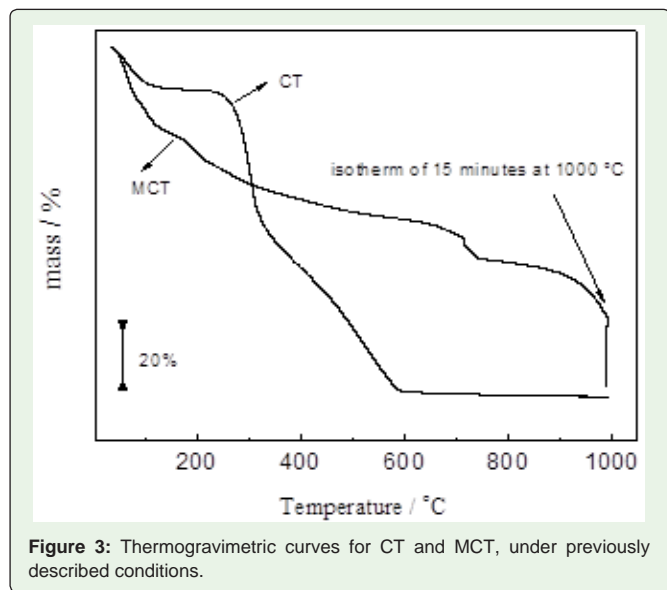


Figure 3: Thermogravimetric curves for CT and MCT, under previously described conditions.

a carbonaceous material. Those findings are in agreement with the studies by Torres (2005) [35], in which the decomposition of chitosan and epichlorohydrin-modified chitosan, prepared by using a dynamic nitrogen atmosphere at a flow rate of 25 mL min⁻¹ and the same heating rate applied in the present study, occurred in two stages, corresponding to dehydration and decomposition.

Moreover, the same number of events was also observed by Santos et al. (2003) [36], using either a dynamic nitrogen atmosphere or a dynamic air atmosphere, in both cases at a flow rate of 90 mL min⁻¹. In the case of the dynamic air atmosphere, decomposition seemed to occur in three stages. According to the authors, the last stage corresponded to the burning of the carbonaceous material generated in the second step.

As seen by comparing the thermograms for both sorbents, modified chitosan decomposes at higher temperatures when compared to pure chitosan, showing an increase in thermal stability due to the generated structural modification.

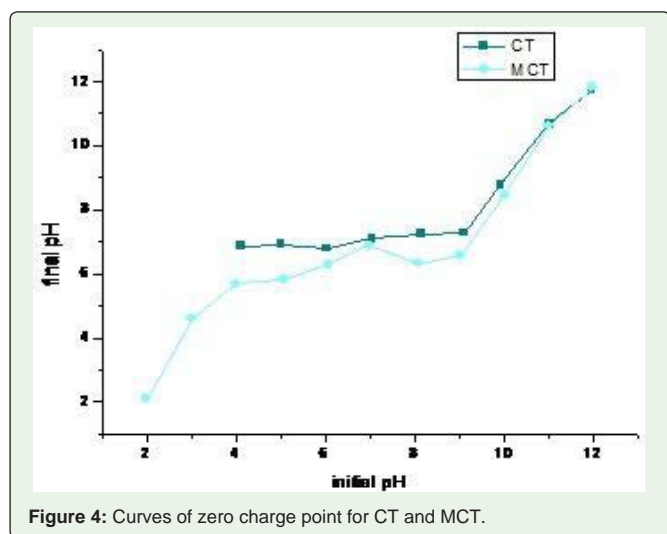


Figure 4: Curves of zero charge point for CT and MCT.

Table 1: Analytical curves and molar absorptivity for MO under experimental conditions, pH = 5, 0; pH = 6, 0; pH = 7, 0; pH = 8, 0 e pH = 10.

pH	Regression/ analytical curve
5.0	$A = 23732C_{MO} + 0.0067$
6.0	$A = 24092 C_{MO} + 0.0030$
7.0	$A = 24988 C_{MO} + 0.0083$
8.0	$A = 23686 C_{MO} + 0.0276$
10.0	$A = 25409 C_{MO} + 0.0101$

The study of ZCP is a simple and useful method used to understand how as the surface charge varies depending on pH of the solution. In this kind of studies, a given mass of sorbent is added to a solution in which the initial pH is adjusted with a strong acid or base. After a period of time, the equilibrium is established and if any interaction occurs the final pH would be different from the initial one. The result of this study is plotted in a graphic “initial pH” versus “final pH”. The ZCP is the pH in which the initial and the final pH are the same. Below the ZCP the superficial charge of the sorbent is positive and above this pH value the superficial charge of this will be negative [34].

As can be seen in Figure 4, the ZCP for CT was 6,5 and for CTM was 7,2. Below these values the superficial charge of both sorbents is positive and in consequence of it the sorption of negative molecules, as MO, is better in these pH values.

Sorption experiments

Analytical curves and modeling: The molecular absorption spectra in the visible region for the dye solutions prepared at pH between 5.0 and 10.0 showed λ_{max} at 465 nm, which was not pH-dependent, in agreement with the value described by Morais (2007) [37], and can be considered a big analytical advantage.

Analytical curves were measured at MO λ_{max} using solutions with concentrations ranging from 9.16×10^{-6} to 6.10×10^{-5} mol L⁻¹. Table 1 presents the regression equations for the calibration, prepared using the different pH values investigated in the present study.

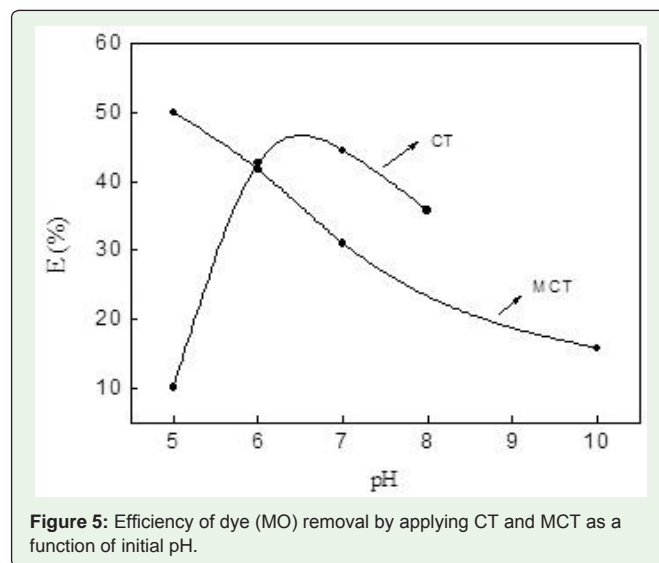


Figure 5: Efficiency of dye (MO) removal by applying CT and MCT as a function of initial pH.

The R² values for all calibration curves were 1.00, indicating a linear relationship between analyte concentrations and absorbances, so the studied concentration range showed no deviations from the Lambert-Beer law.

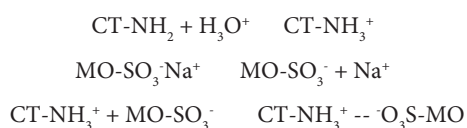
Influence of initial pH and sorption phenomena

Figure 5 shows removal efficiency behavior as a function of the initial pH of the solution. It is easily observed that the MO sorption process onto Chitosan (CT) and Modified Chitosan (MCT) were both pH-dependent.

For modified chitosan, pH increases reflect an almost linear decrease in efficiency, while for raw chitosan maximum efficiency can be observed between pH 6 and 7. The low removal efficiency by CT in acidic media may be related to the solubilization of the sorbent. Further more, pH values higher than 8.0 were not evaluated, since polymer degradation occurred above this value. MCT, however, can be used in acid solutions with pH values of less than 5.0 and in alkaline solutions at pH values greater than 8.0, demonstrating higher chemical stability and a wider range of applications when compared to the raw material.

Chitosan has a pK_a value of around 6. This value depends on the mass and the degree of deacetylation of this amino polysaccharide [24]. As cited previously, protonation of the amino group (CT- NH₃⁺) occurs in acidic media, generating positive charges on the CT surface, thus increasing the initial pH of the solution, in turn reducing the protonation of amino groups by decreasing their interaction with the dye, as seen in Figure 3. A similar reasoning can be inferred for MCT.

MO is an anionic dye, which shows a deprotonated sulfonic cluster (MO-SO₃⁻) in its structure, and, although such a group does not participate in MO acid-base reactions, since reactions actually take place at the nitrogen atoms present in the azo group, they confer a negative charge to the molecule in all assessed pH values. Since the sorbents are positively charged in acidic and neutral solutions, dye sorption can be explained mainly by the electrostatic attraction of the sulfonic group and the colorant present in protonated amino groups, as follows:



Similar sorption behaviors among dyes and chitosan, and even some for chitosan derivatives, have been described in the literature [37]. In addition, despite the significantly reduced dye removal efficiency at pH values above 7.0, MO sorption still occurs with some sorbents at around 36% removal for CT at pH 8.0, and 16% for MCT at pH10.0. The mechanism in this case may not be electrostatic, and may be explained probably exclusively by hydrophobic interactions between the benzene nuclei of the dye and the glycoside units of the sorbent [25,37]. These weaker interactions (compared to those for electrostatic cases) explain the lower sorption observed in the present study.

Higher removal percentages were observed for CT at pH between 6 and 7, of 42% and 44%, respectively. As the observed difference was not significant for the other assays involving this sorbent, the initial pH of the solution was set at pH 6.0. On the other hand, by using

MCT, higher removal percentages were observed with decreasing pH values. The solution whose initial pH was adjusted to 5.0 presented the maximum removal percentage (50%). Because of this, a prior pH adjustment to 5.0 was conducted for the other assays involving this sorbent.

Influence of sorbent mass on dye sorption

Figure 6 (a) illustrates the behavior/relationship between sorbent masses and dye removal efficiency onto CT and MCT particles. The curve profiles as a function of sorbent masses indicated that, for both CT and MCT, removal efficiency increased as a function of sorbent mass in the studied range. For both sorbents, the highest amount of dye removed was associated with a mass of 500mg, which removed about 82% and 67% dye for MCT and CT, respectively.

The increase in the percentage of dye removal due to the increased sorbent mass can be related to the increased surface area of the sorbent, as well as the number of active sites available for dye sorption.

In their study, Cardoso et al. (2011) [13] described the use of the cupuaçu skin as a bio-sorbent for application in the removal of textile dyes from aqueous solutions, also finding that growing sorbent masses has a positive effect on the bleaching of said aqueous solutions containing dyes. However, for asorbent concentration greater than 2.5g L⁻¹, dye removal remained virtually constant, which was not observed in the mass range evaluated in the present study.

The evaluation of the effect of sorbent mass in the sorption capacity (Q) of CT and MCT was also performed. Figure 6(b) illustrates the behavior between masses and sorption capacity for both CT and MCT.

Although the sorption efficiency is favored by increasing the sorbent mass, the same pattern was not observed for sorption capacity. In this case, sorption capacity was enhanced with decreasing sorbent masses. This behavior has also been described by Zhao et al. (2013) in their work on MO sorption in multi-walled carbon nano tubes [39].

The sorption capacity is calculated by measuring the ratio of the mass sorbed on to the sorbent mass. Experimentally, it was observed that, with increasing sorbent masses, sorption is increased, although in a non-linear manner, which explains the decrease in adsorption capacity with increasing masses, while an increase is observed in removal efficiency.

By a mechanistic point of view, one can imagine that the increase in sorbent mass did not generate an equivalent increase in the number of sites available for sorption. Since adsorption is a surface

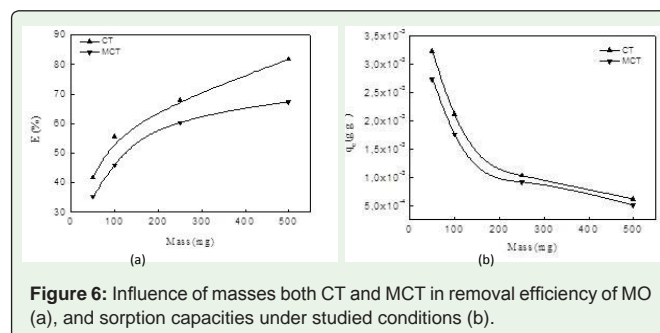


Figure 6: Influence of masses both CT and MCT in removal efficiency of MO (a), and sorption capacities under studied conditions (b).

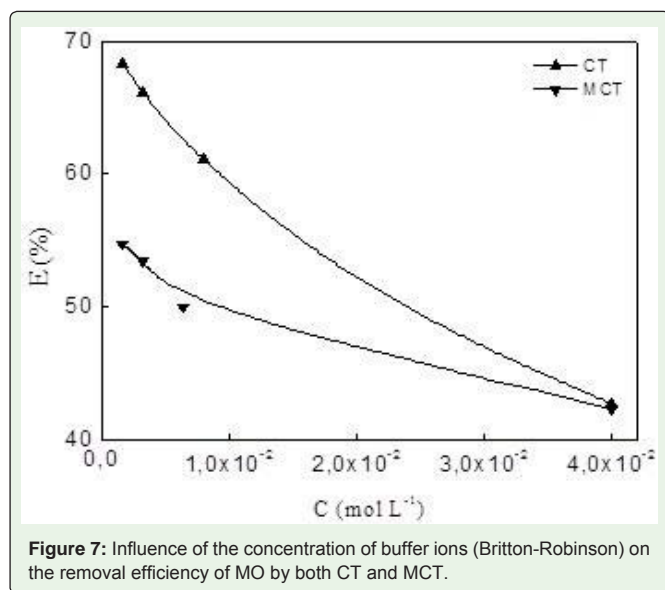


Figure 7: Influence of the concentration of buffer ions (Britton-Robinson) on the removal efficiency of MO by both CT and MCT.

phenomenon, it would be possible to assume that the particles added to the chitosan solution have sites that are unattainable by the solution (since the particles are aggregated). Thus, an absolute increase of sites would occur (since mass was increased), but with a relative decrease of sorption-available sites.

Influence of ionic strength on dye sorption

By analyzing the results obtained in the sorption experiments illustrated in Figure 7, it was observed that, as the concentration of ions of the buffer solution increased (and, consequently, ionic strength), removal efficiency decreased. The removal percentages varied from 43% to 68% for CT, and 42% to 55% for MCT. For CT, greater removal efficiency was associated with the buffer concentration of $1.6 \times 10^{-3} \text{ mol L}^{-1}$, which was subsequently applied in all further experiments. For MCT, the same behavior was observed. However, the buffer concentration was not sufficient to maintain the pH of the system at the desired value. Thus, in the experiments employing MCT, the lowest buffer concentration capable of preventing pH variations in the system was used, of $6.4 \times 10^{-3} \text{ mol L}^{-1}$.

The main dye sorption mechanism is electrostatic. With regard to this mechanism, the presence of high concentrations of other ionic species (PO_4^{3-} , BO_4^{3-} , CH_3CO_2^- , H^+ , Na^+ , K^+ , from the buffer) probably interfere with the equilibrium condition, since negative species, such as dyes, were increasingly surrounded by positive species (H^+ , for example), while positive chitosan sites attracted negative species (PO_4^{3-} , for example), resulting in decreases in the electrostatic interaction between positive chitosan sites and the anionic dye. This ionic strength effect is sometimes called the salt effect [40]. This behavior has also been described by Obeid et al. (2013) [41], in a study regarding methyl orange sorption using a magnetic composite chitosan.

Influence of initial dye concentration on the sorption process

The sorption capacity behavior of CT and MCT, according to the initial dye concentration, is presented in Figure 8. By assessing the q

vs initial MO concentration graph, a linear trend is noted, in which the increasing sorption capacity of the sorbents reflects the increased MO initial concentration. The sorptive capacity increases approximately 10 times with increasing concentrations, from $1.53 \times 10^{-5} \text{ mol L}^{-1}$ to $5.80 \times 10^{-5} \text{ mol L}^{-1}$. This demonstrates that the initial MO concentration shows significant influence on the sorption process.

Similar behavior has been described in the literature for dye sorption on chitosan and modified chitosan [30,39,42]. According to Zhang et al. (2012) [42], the initial dye concentration is responsible for generating the driving force required to overcome the resistance to mass transfer of the solution to the solid phase. Thus, the author suggests that the increase in sorption capacity caused by the increase of the initial dye concentration can be related to an increase in the driving force involved in mass transfer.

From a mechanistic point of view, one can imagine that when maintaining the sorbent mass constant, the number of sites available for sorption will be also kept the same, regardless of the MO concentration. However, as the dye concentration increases, the ratio regarding the amount of MO and the number of active sites seemed to be altered, which can in turn alter the equilibrium position; a greater amount of MO then binds to the solid phase sites, which mathematically represents an increase in sorption capacity.

Still in relation to the mechanism involved in this process, by assessing the dependence between the quantity of sorbed dye and the initial concentration, a possible formation of multiple layers can be suggested in which, after the formation of the first layer of dye, electrostatic interactions between the dye and the sorbent become less relevant to the overall process, while van der Waals interactions become more significant. Accordingly, by increasing the initial concentration, leads to the formation of additional dye layers, even if all sorbed sorption sites located in the sorbent surface are occupied. Thus, as the initial concentration of the sorbate increases, an increase in the sorption capacity is also attained. The results of the present study are strong evidence of such a proposed mechanism.

Kinetics studies

The study of sorption kinetics generates essential information

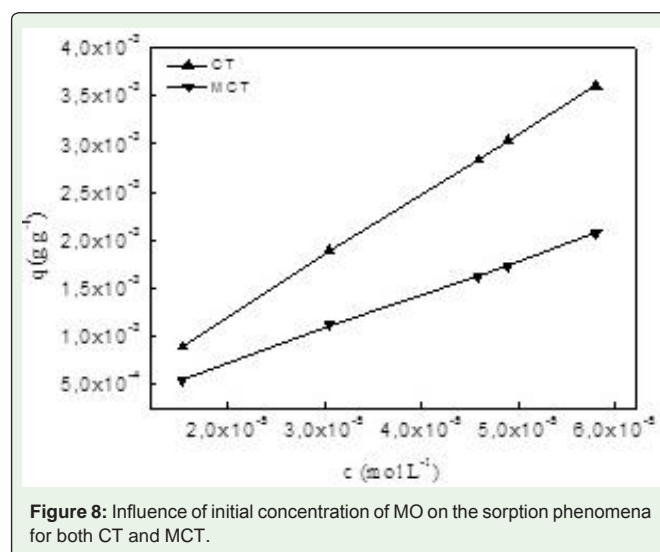
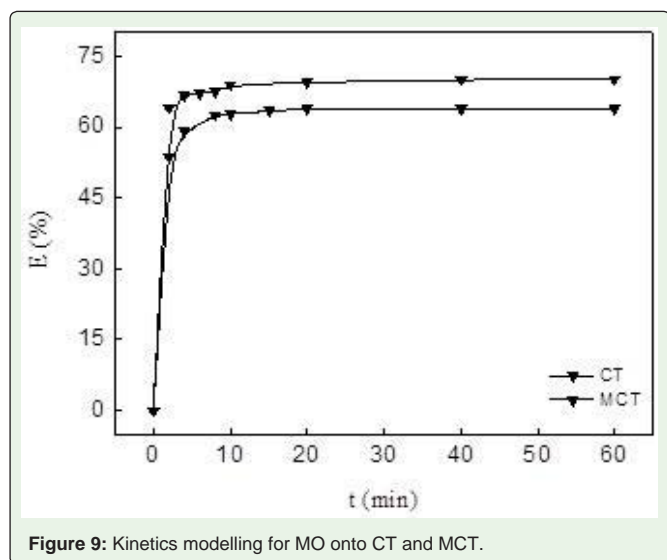


Figure 8: Influence of initial concentration of MO on the sorption phenomena for both CT and MCT.



for model in gand predictions regarding the sorption process. Based on kinetic models, one can achieve the rate of sorption which rules the time of residence in the solid-liquid interface, allowing for calculations on the time required for a given sorption, until it reaches equilibrium. More over, it is possible to identify the influence of the reagents (sorbent and sorvate) in this process.

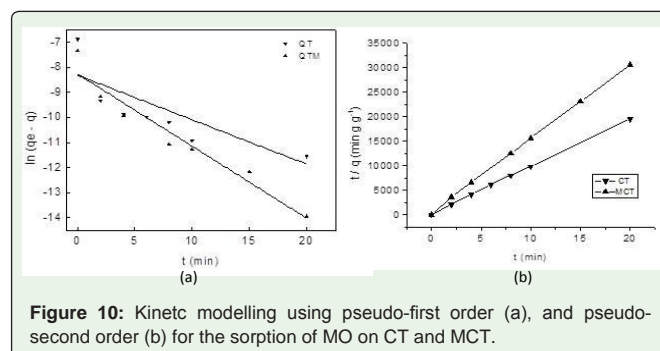
Using the optimal pH and ionic strength conditions, kinetic studies were performed to determine the time required for the system to reach equilibrium. Despite the optimized mass of 500mg, for CT assessments, 250mg were used, while for MCT applications, 100mg were used, due to the fast achievement of sorption equilibrium, which makes modeling difficult.

The MO sorption kinetics on to CT and MCT particles are displayed in Figure 8. The curves indicate that the kinetics equilibria were reached in approximately 10 minutes for both sorbents, remaining constant until the end of the experiment (60 minutes).

In order to exploit the possible kinetic model that best describes the sorption process, experimental data obtained in the sorption experiments were assessed by applying pseudo-first and pseudo-second order models, most frequently used for such purposes (Figure 9).

The $\ln(q_e - q)$ as a function of time graph for the pseudo-first order model (Figure 10 (a)), and t/q as a function of time for the template pseudo-second order model (Figure 10 (b)), which provides a linear relationship, allowed for the calculation of the parameters relating to each template (when the system fit such models). The analysis of the linear correlation coefficients (R^2) obtained indicated that the kinetic model that best represented the experimental data of this study was the pseudo-second order model, with R^2 circa 1.00 for both sorbents.

Another relevant parameter to evaluate the kinetic model which best represents the experimental data is the comparison between the equilibrium sorption capacity, calculated by the kinetic model, and the equilibrium sorption capacity obtained experimentally (Table 2). The q values calculated by the pseudo-second order model were $1.03 \times 10^{-3} \text{ g g}^{-1}$ and $6.59 \times 10^{-3} \text{ g g}^{-1}$ for MCT and CT, respectively. The pseudo-second order q values were very close (in the case of CT, it



the same) to the $q_{e,exp}$ values, representing one more piece of evidence that MO sorption kinetics for the two sorbents followed the pseudo second order model.

Equilibria studies

For the equilibria studies, the initial MO concentrations in the solutions varied from $1.53 \times 10^{-5} \text{ mol L}^{-1}$ to $5.80 \times 10^{-5} \text{ mol L}^{-1}$. For the CT experiments, 250mg were used, with the pH and the ionic strength of the solution (expressed in buffer concentration) set at 6.0 and $1.6 \times 10^{-3} \text{ mol L}^{-1}$, respectively. For the MCT experiments, 100mg were used and the study was conducted in pH 5.0 with final buffer concentration of $6.4 \times 10^{-3} \text{ mol L}^{-1}$.

A suitable assessment of the experimental data obtained at equilibrium conditions is of paramount importance to evaluate sorbent properties. Balance studies allow for calculations regarding the sorption capacity of the sorbent, which can then be used to build sorption isotherms that provide information regarding surface properties and the affinity between the sorbent and the sorvate.

Among the mathematical models described in the literature that correlate the amount of a sorbent sorbed in equilibrium with the solution, the most commonly used to delineate the sorptive properties of the sorbent used in specifically in dye sorption are the Langmuir and Freundlich models.

The plotting of $\ln q_e$ vs $\ln c_e$ as per the model described by Freundlich, and c/q vs c_e provide a linear relationship for calculating the parameters for each model. Through the analysis of the linear correlation coefficients (R^2) obtained, it was possible to identify the isotherm model that best represented the experimental data of the present study. Figure 11 displays the Langmuir and Freundlich isotherms obtained for CT and MCT.

Table 2: Kinetics parameters found to the sorption of MO on CT and MCT.

Kinetic model	Parameters	CT	MCT
Pseudo-first order	$q_{e, exp.} (\text{g g}^{-1})$	1.03×10^{-3}	6.54×10^{-4}
	$q_{e, calc.} (\text{g g}^{-1})$	2.43×10^{-4}	2.55×10^{-4}
	$K_1 (\text{min}^{-1})$	0.1776	0.2858
	R^2	0.690	0.926
Pseudo-second order	$q_{e, exp.} (\text{g g}^{-1})$	1.03×10^{-3}	6.54×10^{-4}
	$q_{e, calc.} (\text{g g}^{-1})$	1.03×10^{-3}	6.59×10^{-4}
	$K_2 (\text{min g g}^{-1})$	6364	6098
	R^2	1.00	1.00

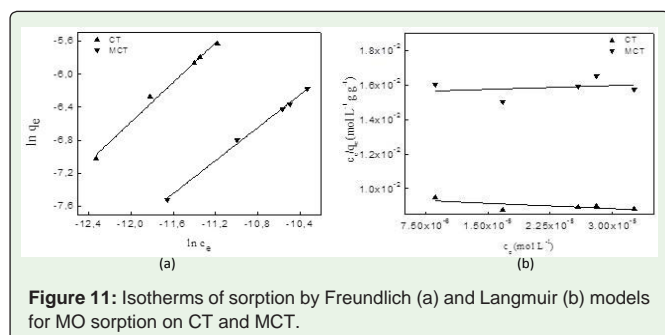


Figure 11: Isotherms of sorption by Freundlich (a) and Langmuir (b) models for MO sorption on CT and MCT.

According to the analysis of the obtained R^2 values for both sorbents, the model that best represents the experimental data for both the CT and for the MCT was the Freundlich isotherm. The parameters calculated for this model are shown in Table (3). The Langmuir isotherm parameters were not calculated because the R^2 values for CT and MCT were lower than 0.400.

Regarding the maximum sorption capacity calculated from the Freundlich isotherm, a decrease of this capacity is related to sorbent modification. The constant related to the sorption capacity calculated from the Freundlich isotherm m for CT was found to be 2556 g^{-1} , higher than that observed for the MCT, of 61.84 g^{-1} .

The Freundlich model assumes that the surface of the sorbent is energetically heterogeneous. To assess the degree of heterogeneity of energy sorption sites, the surface heterogeneity factor ($1/n$) is used. The lower the value of $1/n$, the more heterogeneous the surface is. Comparing the values obtained for CT and MCT, it is observed that the modification of the surface is more heterogeneous in pure chitosan (Table 3).

The sorption rate (n) can be evaluated by the values calculated after applying the experimental data to the Freundlich model. The higher the value of n , the stronger the interaction between the sorbent and sorbate is. As seen in Table 3, the value associated to MCT is higher than that found for CT, indicating that, although the maximum sorption capacity decreased after modification, the interaction of modified chitosan sorption sites with methyl orange is greater.

Since the sorption process for both sorbents is best shown by the Freundlich isotherm, it becomes possible to infer, based on the theoretical understanding of such a model, that MO sorption in these sorbents is reversible and can occur forming multiple layers.

The formation mechanism of the multiple layers, indicated by the best fit to the Freundlich isotherm, can be explained based on, at least, two aspects:

First, after the formation of the first layer, subsequent layer formation occurs by the interaction between the positive charge

Table 3: Parameters calculated by using Freundlich isotherm for MO sorption on CT and MCT.

Parameter	CT	MCT
$1/n$	1.202	0.998
N	0.832	1.00
$K_{ad} (\text{g}^{-1})$	2556	61.84
R^2	0.988	0.997

present in the protonated zodye (which is present in the solution due to the balance of the dye-involved protonation reaction) and the negative charge of the sulfonate group.

Secondly, after the formation of the first layer, the dye molecules will be attracted to the adsorbent by van der Waals electrostatic interactions. The multiple layers will then be formed through hydrophobic interactions between the aromatic rings present in the dye structure.

A similar discussion regarding the formation of multiple sorption layers of the same dye in chitosan modified by glutaraldehyde was carried out by Morais (2008). The author discussed data obtained in a study of the equilibrium relations involved in the sorption process and the measurement of zeta potential as a function of the pH of the continuous phase. According to the study, sorption at low concentrations is described by the Freundlich model. Furthermore, the concentration of the dye and pH decrease favor sorption, with an adsorption capacity of 0.131 g^{-1} and 88% retention percentage at pH 5.0.

Conclusion

The modified chitosan synthesized in this work proved to be an excellent sorbent for methyl orange, a simple structured azodye. This result can serve as a basis for sorption studies of other dyes in the same class, as well as other negatively charged substances.

The maximum adsorption capacity of the modified chitosan obtained in the present study was of 61.84 g^{-1} at pH 5.0, lower than for pure chitosan, of 2556 g^{-1} . However, the reduction of the sorption capacity was compensated by relevant gains in thermal and chemical resistance after modification.

The fact that the dye sorption followed a kinetic pseudo-second order model is in agreement with the results reported in the literature for dye sorption by biosorbents.

According to the sorption experiments conducted in the present study, increasing pH and ionic strength have a negative influence on dye removal efficiency, by leading to a decrease in sorbent removal, while increasing sorbent mass presents the opposite effect, of increasing removal efficiency. The initial concentration of the dye, in turn, significantly increases sorption capacity.

Regarding the equilibrium studies, the isotherm that best represented the experimental data was the Freundlich isotherm, suggesting the formation of multiple layers. As observed in the present study, the increase in sorption when reducing pH and ionic strength indicates that the sorption mechanism involves electrostatic interactions between the negatively charged dye and the positively charged sorbent.

References

- Fu F, Wang Q. Removal of heavy metal ions from waste waters: a review. *J Environ Manage.* 2011; 92: 407-418.
- Crini G. Recent developments in polysaccharide-based materials used as adsorbents in wastewater treatment, *Progress in Polymer Science.* 2005; 30: 38-70.
- Kunz A, Peralta-Zamora P, Moraes SG, Durán N. Novas tendências no tratamento de efluentes têxteis, *Química nova.* 2002; 1: 78-82.
- Szygula A, Guibal E, Ruiz M, Sastre A. The removal of sulfonated azo-dyes by coagulation with chitosan, *Colloids and Surfaces A: Physicochem, Eng. Aspects.* 2008; 330: 219-226.

5. Islam JMM, Habib SMA, Parvin F, Rahman MF, Saadat AHM, Khan MA. Removal of Industrial Dye Effluent (Drimarene Yellow) by Renewable Natural Resources, *American Academic & Scholarly Research Journal*. 2013; 5: 144-150.
6. Kaushik CP, Ravinder T, Kaushik N, Sharma JK. Minimization of organic chemical load in direct dyes effluent using low cost adsorbents, *Chemical engineering journal*. 2009; 155: 234-240.
7. Rafatullah M, Sulaiman O, Hashim R, Ahmad A. Adsorption of methylene blue on low-cost adsorbents: a review, *Journal of Hazardous Materials*. 2010; 177: 70-80.
8. Guzel F, Saygili H, Saygili GA, Koyuncu F. New low-cost nanoporous carbonaceous adsorbent developed from carob (*Ceratonia siliqua*) processing industry waste for the adsorption of anionic textile dye: Characterization, equilibrium and kinetic modeling, *Journal of molecular liquids*. 2015; 206: 244 - 255.
9. Jin ZH, Firoozabadi A. Effect of water on methane and carbon dioxide sorption in clay minerals by Monte Carlo simulations, *Fluid Phase Equilibria*. 2014; 382: 10-20.
10. Musso TB, Parolo ME, Pettinari G, Francisca FM. Cu (II) and Zn(II) adsorption capacity of three different clay liner material, *Journal of Environmental Management*. 2014; 146: 50-58.
11. Gordienko PS, Yarusova SB, Suponina AP, Yakimenko LV. Sorption of Cd²⁺ ions by silicate materials of different origins, *Russian Journal of General Chemistry*. 2014; 83: 2709-2714.
12. Christil I, Brechbuhl Y, Graf M, Kretzschmar R. Polymerization of silicate on hematite surfaces and its influence on arsenic sorption, *Environmental science and technology*. 2012; 46: 13235-13243.
13. Cardoso NF, Lima EC, Pinto IS, Amavisca CV, Royer B, Pinto RB, et al. Application of cupuassu shell as biosorbent for the removal of textile dyes from aqueous solution, *Journal of environmental management*. 2011; 92: 1237-1247.
14. Koduru JR, Chang YY, Kim IS. Low-cost *Schizandra chinensis* fruit peel for Co (II) removal from aqueous environment: Adsorption properties and mechanism, *Asian Journal of Chemistry*. 2014; 26: 289-287.
15. Cutillas-Barreiro L, Ansias-Manso L, Fernández-Calviño D, Nóvoa-Muñoz JC, Fernández-Sanjurjo MJ, Álvarez-Rodríguez E, et al. Pine bark as bio-adsorbent for Cd, Cu, Ni, Pb and Zn: Batch-type and stirred flow chamber experiments, *Journal of Environmental Management*. 2014; 144: 258-264.
16. Su PP, Kim Granholm, Andrey Pranovich, Leo Harju, Bjarne Holmbom, Ari Ivaska. Sorption of metal ions from aqueous solution to spruce bark, *Wood Science and Technology*. 2013; 47: 1083-1097.
17. Kalpana P, King P. Biosorption of Malachite Green Dye on to *Araucaria cookii* bark: Optimization using response surface methodology, *Asian Journal of Chemistry*. 2014; 26: 75-81.
18. Vieira AP, Santana SA, Bezerra CW, Silva HA, Chaves JA, Melo JC, et al. Kinetics and thermodynamics of textile dye adsorption from aqueous solutions using babassu coconut mesocarp, *Journal of Hazardous Materials*. 2009; 166: 1272-1278.
19. Santana SAA, Vieira AP, Silva Filho EC, Melo JCP, Airoidi C. Immobilization of ethylenesulfide on babassu coconut epicarp and mesocarp for divalent cation sorption, *Journal of Hazardous Materials*. 2010; 174: 714-719.
20. Vieira AP, Santana SAA, Bezerra CWB, Silva HAS, Chaves JAP, Melo JAP, et al. Epicarp and mesocarp of babaçu (*Orbignya speciosa*): Characterization and Application in Copper Phtalocyanine Dye Removal, *Journal of Brazilian Society*. 2011; 22: 21-29.
21. Ali N, Hameed A, Ahmed S. Physicochemical characterization and Bioremediation perspective of textile effluent, dyes and metals by indigenous Bacteria, *Journal of hazardous material*. 2009; 164: 322-328.
22. Kalantari H, Yaghmaei S, Rootstaazad R, Mohammad-Beigi H. Removal of zirconium from aqueous solution by *Aspergillus niger*. *Scientia Iranica*. 2014; 21: 772-780.
23. Bhartnagar A, Sillanpää M. Applications of chitin and chitosan derivatives for the detoxification of water and waste water A short review, *Advances in Colloid and Interface Science*. 2009; 152: 26-38.
24. Crini G, Badot PM. Application of chitosan, a natural aminopolysaccharide, for dye removal from aqueous solutions by adsorption processes using batch studies: a review of recent literature, *Progress in Polymer Science*. 2008; 33: 399-447.
25. Kimura IY, Gonçalves AC, Stolberg J, Laranjeira MCM, Fávère VT. Efeito do pH e do tempo de contato na sorção de corantes reativos por microesferas de quitosana, *Polímeros: ciência e tecnologia*. 1999; 51-57.
26. Vakili M, Rafatullah M, Salamatinia B, Abdullah AZ, Ibrahim MH, Tan KB, et al. Application of chitosan and its derivative as adsorbents for dye removal from water and waste water: a review, *Carbohydrate Polymers*. 2014; 113: 115-130.
27. Chen AH, Liu SC, Chen CY. Comparative adsorption of Cu (II), Zn (II), and Pb (II) ions in aqueous solution on the cross linked chitosan with epichlorohydrin, *Journal of Hazardous Materials*. 2008; 154: 184-191.
28. Gonsalves AA, Araújo CRM, Soares NA, Goulart MOF, Abreu FC. Diferentes Estratégias para Reticulação de Quitosana, *Química Nova, São Paulo*. 2011; 34: 1215-1223.
29. Chiou MS, Li HY. Equilibrium and kinetic modeling of adsorption of reactive dye on cross-linked chitosan beads, *Journal of hazardous materials*. 2002; 93: 233-248.
30. Chiou MS, Ho P, Li HY. Adsorption behavior of reactive dyes in aqueous solutions on chemical cross-linked chitosan beads, *Chemosphere*. 2003; 50: 1095-1105.
31. Chiou MS, Ho P, Li HY. Adsorption of anionic dyes in acid solutions using chemically cross-linked chitosan beads, *Dyes and pigments*. 2004; 60: 69-84.
32. McMurry J. *Química Orgânica. LTC - Livros Técnicos e Científicos, Rio de Janeiro*. 1997.
33. Kamari A, Wan Ngah WS, Chong MY, Cheah ML. Sorption of acid dyes onto GLA and H₂SO₄ cross-linked chitosan beads, *Desalination*. 2009; 249: 1180-1189.
34. Fiol N, Villaescusa I. Determination of sorbent point zero charge: usefulness in sorption studies. *Environmental Chemistry Letters*. 2009; 7: 79-84.
35. Torres MA, Vieira RS, Beppu MM, Santana SS. Produção e caracterização de microesferas de quitosana modificadas quimicamente, *Polímeros: ciência e tecnologia*. 2005; 15: 306-312.
36. Santos JE, Soares JP, Dockal ER, Campana Filho SP, Cavalheiro ETG. Caracterização de quitosanas comerciais de diferentes origens, *Polímeros: ciência e tecnologia*. 2003; 15: 242-249.
37. Morais WA, Fernandes ALP, Dantas TNC, Pereira MR, Fonseca JLC. Sorption studies of a model anionic dye on cross linked chitosan. *Colloids and Surfaces A: Physicochem. Eng Aspects*. 2007; 310: 20-31.
38. Morais WA, Almeida AL, Pereira MR, Fonseca JL. Equilibrium and kinetic analysis of methyl orange sorption on chitosan spheres, *Carbohydrate research*. 2008; 343: 2489-2493.
39. Zhao D, Zhang W, Chen C, Wang X. Adsorption of methyl orange dye onto multi walled carbon nanotubes, *Procedia environmental sciences*. 2013; 18: 890-895.
40. Skoog DA, West DM, Holler FJ, Stanley RC. *Fundamentos da Química Analítica, Tradução da 8ª edição norte americana*. São Paulo Ed. Thomson. 2007.
41. Obeid L, Bée A, Talbot D, Jaafar SB, Dupuis V, Abramson S, et al. Chitosan/maghemite composite: a magisorbent for the adsorption of methyl orange, *Journal of colloid and interface science*. 2013; 410: 52-58.
42. Zhang J, Zhou Q, Ou L. Kinetic, isotherm, and thermodynamic studies of adsorption of methyl orange from aqueous solution by chitosan/ alumina composite, *Journal of Chemical and Engineering Data*. 2012; 57: 412-419.